Published in final edited form as:
Invest Ophthalmol Vis Sci. 2009 February ; 50(2): 634–643. doi:10.1167/iovs.08-2277.

Optical effects of anti-TGFβ treatment after photorefractive keratectomy in a cat model

Jens Bühren, MD[1], **Lana Nagy, BS**[1,2], **Jennifer N. Swanton, BS**[1], **Shawn Kenner, BS**[1,3], **Scott MacRae, MD**[1,2], **Richard P. Phipps, PhD**[1,4], and **Krystel R. Huxlin, PhD**[1,2]

[1]University of Rochester Eye Institute, University of Rochester, Rochester NY.

[2]Center for Visual Science, University of Rochester, Rochester NY.

[3]Institute for Optics, University of Rochester, Rochester NY.

[4]Department for Environmental Medicine, University of Rochester, Rochester NY.

Abstract

Purpose—To assess the contribution of corneal myofibroblasts to optical changes induced by photorefractive keratectomy (PRK) in a cat model.

Methods—First, we tested the transforming growth factor β (TGFβ)-dependence of feline corneal keratocyte differentiation into α-smooth muscle actin (αSMA)-positive myofibroblasts *in vitro*. Twenty-nine eyes from 16 cats were then treated with −10D PRK *in vivo* and divided into two post-operative treatment groups: (1) eyes that received 100μg anti-TGFβ antibody for 7 days, followed by 50μg Dexamethasone for another 7 days to inhibit myofibroblast differentiation; (2) eyes that received vehicle solution for 14 days (controls). Corneal thickness and reflectivity were measured by optical coherence tomography. Wavefront sensing was performed in the awake-behaving state pre-operatively and 2, 4, 8 and 12 weeks post-operatively. Wound healing was monitored using *in vivo* confocal imaging and postmortem αSMA immunohistochemistry.

Results—In culture, TGFβ caused cat corneal keratocytes to differentiate into αSMA-positive myofibroblasts, an effect that was blocked by co-incubation with anti-TGFβ antibody. *In vivo*, anti-TGFβ treatment post-PRK resulted in less αSMA immunoreactivity in the sub-ablation stroma, lower corneal reflectivity, less stromal re-growth and lower non-spherical, higher order aberration (HOA) induction than controls. However, there were no inter-group differences in epithelial regeneration or lower order aberration changes.

Conclusions—Anti-TGFβ treatment reduced feline myofibroblast differentiation *in vitro* and following PRK. It also decreased corneal haze and fine-grained irregularities in ocular wavefront after PRK, suggesting that attenuation of the differentiation of keratocytes into myofibroblasts can significantly enhance optical quality after refractive surface ablations.

Keywords

laser refractive surgery; wavefront aberrations; optical quality; steroids; wound healing; myofibroblasts; keratocytes

Correspondence and reprint requests: Dr. Krystel R. Huxlin, PhD, Department of Ophthalmology, Box 314; University of Rochester Medical Center; 601 Elmwood Ave, Rochester, NY 14642, USA; phone +1-(585) 275−5495; email: huxlin@cvs.rochester.edu.
The authors have no proprietary interest in any devices used in this study.
Dr. MacRae has acted as scientific consultant to Bausch & Lomb, Inc.

Increasing awareness of the potential risk of iatrogenic keratectasia after laser *in situ* keratomileusis (LASIK) has led to a renewed interest in photorefractive keratectomy (PRK) and prompted the development of advanced surface ablation techniques like laser subepithelial keratomileusis (LASEK)[1] and Epi-LASIK[2]. One major disadvantage of surface ablations over LASIK is the more pronounced wound healing response, whose functional consequences include a longer visual rehabilitation period, regression and haze. Since these side effects can significantly limit the treatment of higher myopia (reviewed in[3-5]), several attempts have been made to decrease their occurrence through preservation of the epithelial layer (*e.g.* LASEK and Epi-LASIK) and pharmacological modulation of wound healing, as proposed in the early days of PRK[6]. Topical steroids have been used widely[7], but their effects on haze and refractive regression remain controversial[8-11]. Mitomycin C, a cytostatic agent originally introduced for chemotherapy of malignant tumors, has also been shown to attenuate wound healing after PRK, particularly in cases with higher susceptibility for regression and haze, *i.e.* those involving the treatment of higher myopia[12-15]. However, safety concerns and side effects have afflicted the use of steroids (elevation of intraocular pressure, cataract induction and delayed epithelial healing) and Mitomycin C (cytotoxic, possibly mutagenic, limited data on long-term keratocyte integrity), prompting the search for alternatives.

One means of modulating corneal wound-healing is via the inhibition of transforming growth factor β (TGFβ)[16, 17]. TGFβ is a multifunctional cytokine released by the lacrimal gland, the corneal epithelium and conjunctival cells[18]. TGFβ promotes keratocyte proliferation[19, 20], migration[21], differentiation into myofibroblasts that express α-smooth muscle actin (αSMA - reviewed in[22]) and the deposition of extracellular matrix proteins[19]. TGFβ has been shown to play a crucial role in the development of haze after PRK, so that application of anti-TGFβ antibodies to the eye reduces both corneal reflectivity (haze) and fibrosis after PRK in rabbits[16, 17]. However, stromal re-growth still occurred, suggesting that at least in the rabbit, stromal regeneration may be controlled by TGFβ-independent mechanisms[17].

Other than haze, the optical consequences of blocking TGFβ after PRK[16, 17] have never yet been examined. The cat model used in the present study is unique in allowing simultaneous investigation of biological and optical aspects of corneal wound healing after PRK[23-25]. However, before testing the *in situ* effects of anti-TGFβ treatment in the cat, we first measured the response of feline corneal keratocytes to TGFβ stimulation *in vitro,* to verify that they behaved similarly to keratocytes from rabbits, pigs and humans. *In vivo* experiment were then carried out to test the hypothesis that blocking TGFβ activity in the cat eye after PRK: (1) decreases transformation of corneal keratocytes into contractile myofibroblasts, (2) decreases haze (corneal reflectivity) by reducing the incidence of reflective myofibroblasts in the ablation optical zone, (3) decreases refractive regression by slowing keratocyte proliferation and the generation of new extracellular matrix in the stroma, and (4) decreases the induction of higher order aberrations (HOAs) by decreasing the fine-grained, contractile influence of myofibroblasts on the corneal surface.

Materials and methods

All animal procedures were conducted according to the guidelines of the University of Rochester Committee on Animal Research (UCAR), the ARVO Statement for the Use of Animals in Ophthalmic and Vision Research, and the NIH Guide for the Care and Use of Laboratory Animals.

Cell culture experiments

Corneal keratocytes were isolated from four normal, adult domestic short-hair cats, as previously described[22, 26-28]. Cells were plated on both 1mm collagen IV-coated glass coverslips and 6-well collagen IV-coated tissue culture plates (VWR International, West

Chester, Pa.). Cells were seeded at a density of 10^5 cells per well and cultured in 1x PenStrep, gentamicin, 1x Dulbecco's Modified Eagle Medium:Nutrient Mix F-12 (D-MEM/F-12) (1X) liquid, 1:1 Contains L-glutamine, but no HEPES buffer or phenol red (Invitrogen, Carlsbad, Calif.). When the first batch of cells approached 80% confluence, they were exposed to recombinant human TGFβ (Calbiochem, San Diego, Calif.) ranging in concentration from 0 −10ng·mL^{-1} in order to assess whether this factor caused them to differentiate into αSMA-positive myofibroblasts. The optimal dose at which TGFβ induced strong αSMA expression at 72 hrs was 1ng·mL^{-1}. New sets of primary feline corneal keratocytes were then incubated with a combination of 1 ng·mL^{-1} TGFβ and neutralizing mouse monoclonal anti-TGFβ antibody (Clone 1D11, R&D Systems, Minneapolis, Min.) ranging in concentration from 0 −2ng·mL^{-1}. After 72 hrs in culture, the experiment was stopped to assess what dose of antibody blocked TGFβ-dependent induction of myofibroblast differentiation, as measured via αSMA expression. All cell culture experiments were repeated three times.

Immunofluorescence—Cultured cat corneal keratocytes plated on coverslips were rinsed once in phosphate buffered saline (PBS), fixed in 4% paraformaldehyde in 0.1M PBS for 6 min at room temperature (25°C). They were then permeabilized by incubation with 0.2% Triton X-100 in 0.1M PBS (Sigma Aldrich, St. Louis, Mo.) for 6 min at 25°C before incubation for 1hr at 37°C with 2μg·mL^{-1} of mouse monoclonal anti-αSMA antibody (clone 1A4, Sigma Aldrich, St. Louis, Mo.). After washing off the primary antibody, the coverslips were incubated with anti-mouse IgG tagged with AlexaFluor® 488 (2μg·mL^{-1}, Molecular Probes, Eugene, Oreg.). Finally, the cells were double-stained with propidium iodide (0.1μg·mL^{-1}, Invitrogen) to identify all nuclei. Coverslips were then mounted onto slides and imagined using 63x objective on a Zeiss LSM510 confocal microscope.

Western blot analysis—Cells were collected from cultures at various time points (0, 24, 48, 72 and 120 hrs) by incubating them for 5 min in 0.05% trypsin with EDTA 4Na (1X, Invitrogen) and spinning them into a pellet before lysis for 10 min at 4°C. The samples were then spun again at 14,000rpm for 10 min at 4°C, the supernatant was collected and protein concentration was determined by measuring absorbance at 280nm using a spectrophotometer. Samples were adjusted to 10μg/well, boiled for 5mins with 4x sample buffer (Invitrogen), then loaded and run on a 1% BisTri Gel (Invitrogen) before being stained for 1hr in Coomassie Blue (BioRad, Hercules, Calif.) to verify equal protein loading for each well. After de-staining overnight, gels were then transferred to nitrocellulose membrane (Invitrogen) and electrophoresed for 1 hr at 25V. The membranes were blocked overnight at room temperature in 5% condensed milk (Nestle Carnation, Wilkes-Barre, Pa.) and incubated for 2h at room temperature in mouse monoclonal anti-αSMA antibody (10μg·mL^{-1}, Sigma Aldrich, St. Louis, Mo.). After washing with PBS, the membranes were incubated with goat anti-mouse HRP conjugate (the Jackson Laboratory, Bar Harbor, Maine). Equal amounts of Western Dura reagents A and B (Pierce, Rockland, lll.) were placed on the blot and incubated for 5 min at room temperature, after which the blot was exposed in BioRad Gel Doc (BioRad, Hercules, Calif.).

In vivo experiments

A list of treatments administered and measurements collected in living cats is provided in Table 1.

PRK surgery—Twenty-nine eyes from 16 normal, domestic short hair cats (*felis cattus*) underwent a conventional spherical PRK for −10 diopters (D) with a 6mm optical zone (OZ) and a 1.55mm transition zone, resulting in a total treatment zone 9.1 mm in diameter and a central ablation depth of 168 μm (Planoscan 4.14; Bausch & Lomb, Rochester, N.Y.). PRK was performed by one of two surgeons (SM, JB) under topical (Proparacaine 0.5%, Falcon,

Fort Worth, Tex.) and surgical anesthesia (Ketamine, 5 mg·kg^{-1}, Medetomedine Hydrochloride 0.08 mg·kg^{-1}), using a Technolas 217 laser (Bausch & Lomb). The ablation was centered to the pupil, which was constricted with two drops of Pilocarpine 3% (Bausch & Lomb).

Anti-TGFβ treatment—Following PRK, 13 eyes received a topical administration of anti-TGFβ antibody (Clone 1D11, R&D Systems, Minneapolis, Minn.). Eleven of these eyes received 50μg of anti-TGFβ twice a day. This was determined to be optimal based on experiments in a separate set of cats (including 2 from this cohort - data not shown) and on results from the literature[16, 17]. The contralateral eyes were treated with vehicle solution (RefreshCelluvisc™, Allergan, Irvine, Calif.) in order to serve as controls. An additional 3 eyes from 3 cats were later added to the control group when a power analysis revealed the need for additional animals to attain statistical significance. For the first application immediately after PRK, both treatment and vehicle solutions were held in place on the cornea using a saturated, sterile, gelatin sponge (Surgifoam™; Ethicon, Piscataway, N.J.) for 2 minutes. Each eye then received a drop of triple antibiotic solution (Neomycin, Polymyxin B Sulphate, Gramicidin Ophthalmic Solution USP, Bausch & Lomb). For the next 7 days, treatment eyes received one drop of 1 mg/ml anti-TGFβ antibody and one drop of antibiotic solution twice a day. Control eyes received one drop of vehicle solution and one drop of antibiotic solution twice a day. During the second post-operative week, treatment eyes received one drop of 0.1% (1mg·mL^{-1}) Dexamethasone suspension (Maxidex™, Alcon) per day. In case of delayed epithelial closure, the first week's treatment was continued until the epithelium closed (usually a couple of extra days). Pain in the early postoperative period was treated using i.v. flunixin meglumine 1.1 mg/kg (Banamine®, Schering-Plough Animal Health, Kenilworth, N.J.) three times/day for three days. Four eyes were excluded from this study: two received a non-optimal dose of anti-TGFβ antibody (as part of dose-response trials), one had a severely de-centered optical zone, and one developed an ulcer and a sequestrum.

Optical coherence tomography—A custom-built, 1310nm anterior segment optical coherence tomographer (OCT) was used to image corneas before and 2, 4, 8 and 12 weeks after PRK. The animals were lightly anesthetized, treated with GenTeal eye gel (Novartis, East Hanover, N.J.) and placed in a head-restraint device to hold their head stable[24]. The OCT recorded a video stream of the central 10mm of cornea at a rate of eight frames per second. Twenty-five corneal images extracted from the video stream were analyzed and averaged per eye and time-point. Custom software was used to measure and calculate the normalized intensity profile across each corneal image, as reported previously[29-31]. Briefly, a rectangular analysis area 105μm wide and spanning the entire thickness of the cornea + gel layer was positioned 1mm nasal to the middle of each corneal image (light grey rectangles in Fig. 4A). This nasal location was chosen to ensure that the same region of cornea was analyzed in all eyes and that it lay outside the area of saturated reflectivity associated with the specular reflection. A profile of pixel intensities was generated across the vertical extent of each analysis area as previously described[29-31]. In order to compensate for fluctuations in laser strength, each profile was normalized by dividing the mean pixel intensity at each vertical pixel location by the mean pixel intensity in the analyzed region of cornea. Finally, the area under the normalized intensity curve was computed for the most superficial 20% of the stroma and expressed as a cumulative intensity value in Fig 4C. The normalized, backscatter intensity profiles were also used to estimate the thickness of the epithelium and stroma from each OCT image. This was done by measuring the vertical difference between intensity peaks within each analysis area[29-31].

In vivo confocal imaging—Confocal imaging of the central cornea was performed in two animals before and 2, 4, 8 and 12 weeks after PRK. Following OCT imaging, the anesthetized

cats were imaged with the Heidelberg Retina Tomographer with the Rostock Cornea Module (Heidelberg Engineering, Dossenheim, Germany). A drop of GenTeal eye gel was placed on each cornea and on the contact cap. Correct alignment was attained, and after setting the focus to the epithelium, several automated scans, each 58μm in depth, were performed until the endothelium became visible. Scans were recorded as digital video sequences and stored on a PC for analysis.

Wavefront analysis in awake-fixating cats—Cats were trained to fixate on single spots of light presented on a computer monitor as previously described[23, 24]. Wavefront measurements were performed in each eye preoperatively and 2, 4, 8 and 12 weeks post-PRK with a custom-built Hartmann-Shack wavefront sensor. The wavefront sensor was aligned to the visual axis of one eye while the other eye fixated a spot on the computer monitor[23]. At least 10 spot array patterns were collected per imaging session per eye. From each spot array pattern, wavefront errors (WFEs) were calculated using a 2^{nd}–10^{th} order Zernike polynomial expansion according to the published standards for reporting aberration data of the eye[32]. The measurements were centered on the ablation OZ by shifting a 6mm centroiding area (analysis pupil) manually to find the wavefront that yielded the most negative C_2^0 value, *i.e.* the maximal treatment effect[25]. For calculation of preoperative WFEs, the analysis pupil was shifted according to the mean offset relative to the pupil center.

Lower-order aberration (LOA) Zernike coefficients were converted into dioptric power vectors (*M*, *J0*, *J45*), where *M* = spherical equivalent, *J0* = 0°/90° and *J45* = 45°/135° astigmatic components. Higher-order aberrations (HOAs) were broken down into coma RMS (the RMS value of all coma terms $C_n^{\pm 1}$), spherical aberration RMS (the RMS value of all coefficients C_n^0) and the RMS of the residual, non-coma, non-spherical aberrations (the RMS value of all remaining HOA $C_n^{\geq |\pm 2|}$). Best theoretical image quality was assessed using Visual Optics Lab (VOL)-Pro 7.14 (Sarver and Associates, Carbondale, Ill.) to calculate the best-corrected visual Strehl ratio based on the optical transfer function (BCVSOTF)[33] for a simulated endpoint of the subjective refraction.

Immunohistochemistry—Two cats were sacrificed at 2 weeks post-PRK, five at 4 weeks post-PRK and four at 12 weeks post-PRK for the purpose of performing corneal histology. Two animals were kept for long-term optical follow-up and no *ex vivo* histology was performed on their corneas. Two separate, normal, adult cats were also sacrificed to serve as un-operated controls. Following euthanasia, corneas were excised and drop-fixed in 1% paraformaldehyde in 0.1M PBS, pH 7.4 for 10 min. They were then transferred to 30% sucrose in 0.1M PBS, and stored at 4°C for 2 days. After embedding in Tissue Tek® O.C.T. Compound (Sakura Finetek, Zoeterwoude, The Netherlands), serial, 20μm thick cross-sections were cut on a cryostat (2800 Frigocut E™; Leica, Nußloch, Germany), mounted on microscope slides and stored in a −20° C freezer until ready to stain.

Slides containing 3 corneal sections each were air dried and rinsed in 0.1M PBS. Two of the sections on each slide were incubated overnight at 4°C with 2μg·mL^{-1} mouse monoclonal anti-αSMA antibody (clone 1A4, Sigma Aldrich, St. Louis, Mo.). The third section was incubated with 0.1M PBS as a negative control. After washing off the primary antibody with 0.1M PBS, the sections were then reacted with anti-mouse IgG tagged with AlexaFluor® 488 (2μg·mL^{-1}, Molecular Probes, Eugene, Oreg.), followed by propidium iodide (0.1μg·mL^{-1}, Invitrogen, Carlsbad, Calif.) to label cell nuclei. The double-labelled sections were imaged using an Olympus AX70 fluorescence microscope and photomicrographs were collected via a high resolution-video camera interfaced with a PC running the ImagePro software (MediaCybernetics, Bethesda, Md.).

Statistical analysis—Inter-group differences in reflectivity, corneal thickness and wavefront aberrations were compared with a paired (or two-sample), two-tailed Student's *t* test. If data were not normally distributed according to a Kolmogorov-Smirnov-Lillefors test, a Wilcoxon-Mann-Whitney *U* test was used instead. Finally, where appropriate, a 2 (condition) × 4 (post-operative time point) mixed factorial ANOVA was also performed. A probability of error of $P<0.05$ was considered statistically significant. All statistical tests were performed using the SPSS 11.0 software package (SPSS Inc., Chicago, Ill.).

Results

Cell culture experiments

Primary cultures of cat corneal keratocytes failed to express αSMA and exhibited a dendritic morphology typical of quiescent corneal keratocytes. When TGFβ was added to the serum-free medium, feline keratocytes altered their morphology, retracting some of their dendritic processes, multiplying and acquiring a distinct myofibroblastic phenotype, which was accompanied by intracellular expression of αSMA after 72 hrs of culture (Fig. 1A). The minimum concentration of TGFβ required for this differentiation and for strong αSMA expression at 72hrs was 1 $ng \cdot mL^{-1}$, as confirmed by immunofluorescence and Western blotting (Fig. 1A and C). Addition of anti-TGFβ antibodies to the incubation medium blocked expression of αSMA in a dose-dependent manner, as shown by immunofluorescence (Fig. 1B) and Western blotting (Fig. 1D).

In vivo experiments

Clinical course and slit lamp findings post-PRK—Of the 10 eyes treated with 1 mg/ml anti-TGFβ twice a day, only one exhibited slightly delayed epithelial healing, which required us to start Dexamethasone treatment 2 days late. All other eyes showed uneventful follow-up, with full epithelial closure by day 7.

In vivo confocal imaging—*Pre-operative examination* showed a regular epithelium and a syncytium of quiescent keratocytes in all eyes (Fig. 2A, E and Fig. 3A, E). *One week after PRK*, the epithelium, though usually closed in eyes treated with anti-TGFβ, appeared hyperplastic and edematous. The superficial stromal was reflective, though hypocellular, with some inflammatory cell infiltrates. The first layer of identifiable keratocytes was found at a depth of 50−100μm below the epithelium. In deeper layers, a fine fiber network and spindle-shaped migratory fibroblasts were visible between the keratocytes. In control eyes, migratory fibroblasts appeared in the hypocellular stroma immediately below the moderately reflective epithelial-stromal interface and keratocytes became identifiable at depths of only 20−30μm below the epithelium. In all eyes, the posterior corneal layers were quiescent, with only occasional migratory fibroblasts observed. The endothelium was inconspicuous in both treatment and control eyes.

Two weeks after PRK, there was increased reflectivity at the epithelial-stromal interface, which was more prominent in control than treated eyes (Fig. 2B, F). The number of migratory fibroblasts increased, with some sprouting processes in both groups. Below the hypocellular zone (10−20μm below the epithelial-stromal interface), activated, reflective keratocytes with distinct cell processes were clustered (Fig. 3B). In control eyes, the epithelial-stromal interface appeared to contain more pronounced cellular elements (Fig. 2F) - likely myofibroblasts - and the layer below the epithelial-stromal interface was populated by activated keratocytes, which appeared more densely packed than in treated eyes (Fig. 3F). The entire layer of activated cells and increased reflectivity was ~90μm thick in both control and anti-TGFβ-treated eyes.

Three and four weeks after PRK, both treatment and control eyes showed further increases in the reflectivity of the epithelial-stromal interface relative to their pre-operative state. Once again, this reflectivity appeared greater in control eyes (Fig. 2C, G). Eyes treated with anti-TGFβ contained some bright stromal cells below the epithelium, but they were less dense than in control eyes and appeared separated by large, optically-clear spaces (Fig. 3C, G). The sub-epithelial layer of activated cells and increased reflectivity now measured ca. 120μm in treated eyes and ca. 90μm in control eyes.

Six, eight and twelve weeks after PRK, the epithelial-stromal interface and the underlying stroma became progressively more similar between treated and control eyes. Both groups displayed decreased interface reflectivity, a layer of stellate, activated, sub-epithelial keratocytes that were arranged in an irregular fashion (Fig. 2D, H) and a denser, deeper meshwork of cells (Fig. 3D, H). Twelve weeks after PRK, the sub-epithelial layer of activated cells and increased reflectivity measured ca. 80μm thick in both anti-TGFβ-treated and control eyes. Apart from the presence of migrating fibroblasts, which became progressively fewer, the posterior stromal layers did not change significantly throughout the observation time and the endothelium remained inconspicuous at all time-points.

Corneal backscatter reflectivity—OCT-derived pre-operative reflectivity of the anterior 20% of the cornea was relatively low and did not differ significantly between cat eyes destined for anti-TGFβ treatment and controls (Fig. 4A-C). PRK increased reflectivity in the anterior 20% of the stroma of both groups ($P<0.05$; Fig. 4A-C). However, this increase was significantly lower in treated than in control eyes, with a peak difference at 4 weeks post-PRK ($P<0.05$; Fig. 4A- C).

Corneal thickness changes—*Pre-operatively*, the mean central corneal thickness of treatment eyes was 587±55μm (control eyes: 582±40μm), the mean stromal thickness was 537 ±67μm (control eyes: 538±52μm) and the mean epithelial thickness was 67±15μm (control eyes: 59±8μm). There were no significant inter-group differences in any of these measures pre-operatively ($P>0.05$; Fig. 4D, E). The epithelial layer was scraped off during PRK, but *two weeks later*, central epithelial thickness had not only regenerated, but in the control group, it was 36±37μm thicker than it had been pre-operatively ($P<0.005$). This did not happen in eyes treated with anti-TGFβ until 4 weeks post-PRK, after which, epithelial thickness decreased back to pre-operative values in both groups (Fig. 4 D). An ANOVA showed no significant effect of treatment or post-operative time on epithelial thickness. PRK removed about 168μm of central stroma. Two weeks later, the central stroma had regenerated half that loss in control eyes, but was still 141±31μm thinner than pre-op in treated eyes ($P<0.01$; Fig. 4E). An ANOVA revealed a main effect of treatment ($F(1,11)=4.96$, $P<0.05$) across the entire post-operative period with control eyes maintaining a significantly thicker stroma post-operatively than eye treated with anti-TGFβ (Fig. 4E).

Ex vivo histology—Normal, un-operated cat corneas exhibited a classical histological structure and a complete absence of αSMA staining within the stroma (Fig. 5). *Two and 4 weeks after PRK*, the sub-ablation zone could be identified by the absence of a clear Bowman's layer, and the expression of αSMA below the epithelium. In control eyes, the band of αSMA immunoreactivity was tick and continuous, while in eyes treated with anti-TGFβ, it formed a much thinner layer, interrupted by αSMA-negative zones (Fig. 5). Qualitative inspection of PI-staining revealed an apparent decrease in keratocyte density following PRK relative to un-operated corneas. However, among PRK-treated corneas, the density of sub-epithelial stromal cells always appeared higher in control corneas than in corneas treated with anti-TGFβ. *Twelve weeks after PRK*, stromal αSMA immunoreactivity decreased relative to its levels 4 weeks post-PRK in both treatment groups. However, PI staining continued to show apparently higher cell density in the sub-ablation zone of control eyes (Fig. 5).

Wavefront analysis—Pre-operatively, there were no statistically significant differences in lower or higher order wavefront aberrations between the two experimental groups ($P>0.05$; Figs. 6 and 7). Two weeks after PRK, the mean change in spherical equivalent was 4.79±0.86 D in the anti-TGFβ group and 5.04±2.11 D in the control group (Table 2; Fig. 6A). Similar amounts of astigmatism (*J0* and *J45*) were induced in the two groups post-PRK ($P>0.05$; Table 2, Fig. 6B, C).

With respect to higher order aberrations, control eyes exhibited a dramatic and significant increase in total higher order RMS (HORMS) 2 weeks post-PRK relative to pre-operative levels ($P<0.05$, Fig. 7A) and a mean decrease of BCVSOTF of 0.67 log units. The HORMS increase was statistically greater in controls than in eyes treated with anti-TGFβ ($P<0.05$, Table 2, Fig. 7A). An ANOVA revealed a main effect of post-PRK time ($F(3,21)=3.38$, $P<0.05$), as well as a significant interaction of time with treatment group for HORMS ($F(3,21)=4.71$, $P<0.05$). Controls also exhibited marked increases in coma, spherical and residual HORMS at 2 weeks post-PRK, which were also significant ($P<0.05$, Fig. 7B, C, D). These aberrations then decreased, with the exception of spherical aberration, which remained high (Fig. 7C). Eyes that received anti-TGFβ treatments did not exhibit the peak increase in higher order aberrations observed in control eyes at 2 weeks post-PRK (Table 2, Fig. 7). Coma, residual and HORMS remained close to pre-operative levels throughout the post-PRK period examined. Only spherical aberration approximated levels attained in controls, particularly at later time-points. A consequence of the greater magnitude of HOA in control eyes was a greater irregularity of the wavefront relative to anti-TGFβ treated eyes. This peaked 2 weeks post-operatively, but was still clearly visible at later time-points (Fig. 8).

Discussion

Several major new findings emerged from the present study. First, cat corneal keratocytes reacted similarly to keratocytes from other species when exposed to TGFβ and its blocking antibodies. Second, following PRK, myofibroblast differentiation in the feline eye could be decreased by topical application of antibodies against TGFβ. Third, decreasing myofibroblast differentiation after PRK significantly decreased non-spherical higher-order aberrations without affecting refractive outcome. In short, the present experiments identify, for the first time, the specific contribution of myofibroblast activity to changes in ocular optics following laser refractive surgery.

Comparative behavior of feline keratocytes in culture

A fundamental finding in the present study is that primary feline corneal keratocytes exhibited a dendritic morphology, lacked αSMA immunoreactivity and reacted to the administration of TGFβ in a manner that was consistent with that of rabbit, human and bovine keratocytes[34-37]. Earlier studies of PRK and other surgical manipulations in animal models suggested that there might be some important inter-species differences in corneal wound healing. One interpretational issue that had to be addressed in the present study was whether any differences in corneal wound healing that emerged from our experiments were related to differential regulation of feline keratocyte behavior by TGFβ. Our cell culture experiments did not support this concept, at least with regard to the TGFβ-regulated differentiation of feline corneal keratocytes into αSMA-positive myofibroblasts. Having established this behavioral baseline *in vitro*, we were able to proceed with *in vivo* experiments, in which the TGFβ regulatory pathway was manipulated following PRK in cats. Specifically, we tested the hypothesis that myofibroblasts, through their contractile ability, are significant contributors to the induction of higher (rather than lower) order ocular aberrations after PRK.

Methodological issues

Unlike prior experiments with neutralizing antibodies against TGFβ in rabbits, *in situ* experiments in cats employed a prolonged, sequential treatment approach with neutralizing antibodies for the first post-operative week and Dexamethasone for a second week (after epithelial closure). Although Dexamethasone reduces $TGF\beta_1$ and $TGF\beta_2$ mRNA levels in healing tissues[38], it was not administered during the first week post-PRK for two reasons: (1) because steroids can impair epithelial closure[39], and (2) because epithelial disruption is a major source of signals for myofibroblast differentiation[40, 41]. Once the epithelium closed, Dexamethasone was administered for an additional week in order to provide a more upstream, prolonged anti-TGFβ treatment effect than antibody application alone[38]. However, differentiation between antibody and steroid action was not the purpose of our study. Thus, control eyes only received vehicle solution and we did not include a third, steroid-only treatment group.

Structural effects of anti-TGFβ *treatment post-PRK*

I*n vivo* confocal imaging and post-mortem histology revealed anti-TGFβ treatment post-PRK to reduce (but not eliminate) the differentiation of cat stromal keratocytes into αSMA-positive myofibroblasts in the sub-ablation zone. A similar effect was previously demonstrated in rabbit models of lamellar keratectomy[16] and PRK[17]. The fact that myofibroblast differentiation could not be suppressed totally is not surprising since it is influenced by both TGFβ-dependent and independent mechanisms[26]. Furthermore, although topically-administered anti-TGFβ antibodies accumulate in the cornea to some extent[16], our application pattern would have created two concentration peaks/day. In contrast, TGFβ was likely released from the injured cornea in a more sustained manner[18, 41-43].

Anti-TGFβ treatment appeared to delay the repopulation of the anterior stroma after PRK. Whether it did so by inhibiting keratocyte migration, proliferation or increasing keratocyte death remains to be determined. The likely effects of anti-TGFβ treatment on the stromal extracellular matrix were not examined in the present study, although some of the differences noted between the thickness of the sub-ablation αSMA positive layer and the thickness of the area of high reflectivity observed on confocal images at 2 weeks post-PRK could be due to both reactive myofibroblasts and the presence of abnormal extracellular matrix. Immunohistochemistry for αSMA, on the other hand, only recognizes the cellular component of this reaction, and when used alone, likely underestimates the extent of “abnormal” or “reactive” stroma in a given piece of tissue.

OCT imaging showed higher reflectivity in the anterior 20% of the stroma in control corneas relative to the treated group throughout the follow-up period, confirming previous results with anti-TGFb treatment in rabbits, which was also shown to decrease reflectivity and haze in the cornea [44-46].

While the epithelial layer regenerated to approximately the same extent in both treatment groups, anti-TGFβ treatment decreased stromal regrowth throughout the post-operative period in the cat. This contrasts with previous results in rabbits treated with the same 1D11 anti-TGFβ antibody, albeit only 3 times/day for 3 days post-PRK[45]. In rabbits, this treatment decreased haze and αSMA expression in the sub-ablation zone, but did not impede stromal regrowth[45]. It is conceivable that the difference in treatment regimen, and to a lesser extent, in method of measuring stromal thickness (OCT in the present study versus confocal microscopy through focusing in Møller-Pedersen et al.'s study [45]), can explain our differing results. However, the possibility remains that cats and rabbits differ in the TGFβ-dependence of cellular mechanisms controlling their stromal regrowth.

Effects of anti-TGFβ treatment on ocular wavefront aberrations post-PRK

The present study showed for the first time, that cat eyes treated with anti-TGFβ post-PRK exhibited greater amounts of non-spherical wavefront aberration patterns than control eyes. While cats exhibit a general under-correction relative to humans when PRK is performed over a 6mm OZ[24], PRK-induced HOAs in the feline model are comparable in magnitude and type to those induced by this procedure in humans[24, 25, 47]. While HORMS, coma RMS and residual HORMS peaked in the early post-PRK period, levels of these higher order aberrations remained at close to pre-operative levels in eyes treated with anti-TGFβ. However, the amount of spherical aberration and lower order aberrations induced by PRK was similar in control eyes and anti-TGFβ-treated eyes throughout the post-operative period. Thus, myofibroblast contractility appears to alter corneal shape in an irregular, non-radially symmetric manner. A possible explanation for this phenomenon is the development of local irregularities in corneal curvature due to small-scale, myofibroblastic contraction of the stroma[48] that remains uncompensated by epithelial filling-in. Interestingly, however, anti-TGFβ treatment did not mitigate the induction of spherical aberration, suggesting this to be a phenomenon dominated by factors that do not significantly implicate myofibroblast differentiation. Previous work suggested that loss of laser ablation efficiency in the corneal periphery and changes in corneal biomechanics might play a more important role in the induction of spherical aberration after laser refractive surgery[49]. What the present data show is that myofibroblast differentiation and contractility are unlikely to contribute significantly to this phenomenon.

Implications for clinical practice

The present experiments were intended as a proof of principle, demonstrating that immediate pharmacological modulation of corneal wound healing post-PRK with agents whose main effect is to block TGFβ activity decreases keratocyte differentiation into contractile myofibroblasts *in situ*. In turn, the decreased incidence of myofibroblasts in the post-PRK cornea led to the attenuation of HOA induction and thus, faster optical rehabilitation after PRK. In contrast to treatment with Mitomycin C, which decreases repopulation of the acellular zone after PRK via non-specific, cytotoxic effects[15], the treatment used in our study was aimed more specifically at the transformation of keratocytes into myofibroblasts. While steroids indirectly block myofibroblast differentiation by down-regulating TGFβ mRNA in the eye, they bear the risk of non-specific side-effects, such as delayed re-epithelialization[39] and increased intraocular pressure (reviewed in[50]). Thus, treatment with anti-TGFβ antibodies in the early post-operative phase following PRK could have the advantage of an immediate myofibroblast blocking action without the side effects of steroids or Mitomycin C. Clinically, a pharmacological treatment that shortens recovery time after PRK is highly desirable because it potentially mitigates the main problems associated with this procedure - wound healing-associated delay of visual recovery and optical instability. On the other hand, such treatment is expensive, requires special handling to avoid antibody degradation and is only partially effective. Ongoing research in our laboratory is focusing on alternative, non-immunogenic substances to specifically block other aspects of myofibroblast function via both TGFβ- and non-TGFβ-regulated pathways.

In summary, our results demonstrate that reduction of myofibroblast differentiation post-PRK decreases HOA induction and consequently, increases retinal image quality. By improving visual outcome, pharmacological modulation of corneal wound healing with myofibroblast-blocking agents could strengthen the value and feasibility of surface ablation procedures as an alternative to lamellar procedures like LASIK.

Acknowledgments

This project was supported by the National Institute of Health (NIH, R01 EY015836 to KRH, Core grant P0EY01319F to the Center for Visual Science), grants from Bausch & Lomb Inc., and the University of Rochester's Center for Electronic Imaging Systems, a NYSTAR-designated Center for Advanced Technology, a grant from the Deutsche Forschungsgemeinschaft (DFG, Bu2163/1-1 to JB) and an unrestricted grant to the University of Rochester's Department of Ophthalmology from the Research to Prevent Blindness Foundation, Inc.

References

1. Azar DT, Ang RT, Lee JB, et al. Laser subepithelial keratomileusis: electron microscopy and visual outcomes of flap photorefractive keratectomy. Curr Opin Ophthalmol 2001;12:323–328. [PubMed: 11507348]
2. Pallikaris IG, Katsanevaki VJ, Kalyvianaki MI, Naoumidi II. Advances in subepithelial excimer refractive surgery techniques: Epi-LASIK. Curr Opin Ophthalmol 2003;14:207–212. [PubMed: 12888719]
3. Wilson SE. Analysis of the keratocyte apoptosis, keratocyte proliferation, and myofibroblast transformation responses after photorefractive keratectomy and laser in situ keratomileusis. Trans Am Ophthalmol Soc 2002;100:411–433. [PubMed: 12545703]
4. Netto MV, Mohan RR, Ambrosio R Jr. Hutcheon AE, Zieske JD, Wilson SE. Wound healing in the cornea: a review of refractive surgery complications and new prospects for therapy. Cornea 2005;24:509–522. [PubMed: 15968154]
5. Dupps WJ Jr. Wilson SE. Biomechanics and wound healing in the cornea. Exp Eye Res 2006;83:709–720. [PubMed: 16720023]
6. Talamo JH, Gollamudi S, Green WR, De La Cruz Z, Filatov V, Stark WJ. Modulation of corneal wound healing after excimer laser keratomileusis using topical mitomycin C and steroids. Arch Ophthalmol 1991;109:1141–1146. [PubMed: 1907822]
7. Arshinoff SA, Mills MD, Haber S. Pharmacotherapy of photorefractive keratectomy. Journal of Cataract and Refractive Surgery 1996;22:1037–1044. [PubMed: 8915800]
8. Gartry DS, Kerr Muir M, Marshall J. The effect of topical corticosteroids on refraction and corneal haze following excimer laser treatment of myopia: an update. A prospective, randomised, double-masked study. Eye 1993;7(Pt 4):584–590. [PubMed: 8253244]
9. Corbett MC, O'Brart DP, Marshall J. Do topical corticosteroids have a role following excimer laser photorefractive keratectomy? J Refract Surg 1995;11:380–387. [PubMed: 8528917]
10. Baek SH, Chang JH, Choi SY, Kim WJ, Lee JH. The effect of topical corticosteroids on refractive outcome and corneal haze after photorefractive keratectomy. J Refract Surg 1997;13:644–652. [PubMed: 9427202]
11. Vetrugno M, Maino A, Quaranta GM, Cardia L. The effect of early steroid treatment after PRK on clinical and refractive outcomes. Acta Ophthalmol Scand 2001;79:23–27. [PubMed: 11167281]
12. Schipper I, Suppelt C, Gebbers JO. Mitomycin C reduces scar formation after excimer laser (193 nm) photorefractive keratectomy in rabbits. Eye 1997;11(Pt 5):649–655. [PubMed: 9474312]
13. Kim TI, Pak JH, Lee SY, Tchah H. Mitomycin C-induced reduction of keratocytes and fibroblasts after photorefractive keratectomy. Invest Ophthalmol Vis Sci 2004;45:2978–2984. [PubMed: 15326110]
14. Gambato C, Ghirlando A, Moretto E, Busato F, Midena E. Mitomycin C modulation of corneal wound healing after photorefractive keratectomy in highly myopic eyes. Ophthalmology 2005;112:208–218. [PubMed: 15691552]discussion 219
15. Netto MV, Mohan RR, Sinha S, Sharma A, Gupta PC, Wilson SE. Effect of prophylactic and therapeutic mitomycin C on corneal apoptosis, cellular proliferation, haze, and long-term keratocyte density in rabbits. J Refract Surg 2006;22:562–574. [PubMed: 16805119]
16. Jester J, Barry-Lane P, Petroll W, Olsen D, HD C. Inhibition of corneal fibrosis by topical application of blocking antibodies to TGF beta in the rabbit. Cornea 1997;16:177–187. [PubMed: 9071531]
17. Møller-Pedersen T, Cavanagh H, Petroll W, Jester J. Neutralizing antibody to TGFbeta modulates stromal fibrosis but not regression of photoablative effect following PRK. Current Eye Research 1998;17:736–747. [PubMed: 9678420]

18. Vesaluoma M, Teppo AM, Gronhagen-Riska C, Tervo T. Release of TGF-beta 1 and VEGF in tears following photorefractive keratectomy. Curr Eye Res 1997;16:19–25. [PubMed: 9043819]
19. Ohji M, SundarRaj N, Thoft RA. Transforming growth factor-beta stimulates collagen and fibronectin synthesis by human corneal stromal fibroblasts in vitro. Curr Eye Res 1993;12:703–709. [PubMed: 8222730]
20. Jester J, Petroll W, Barry P, Cavanagh H. Expression of alpha-smooth muscle (alpha-SM) actin during corneal stromal wound healing. Invest Ophthalmol Vis Sci 1995;36:809–819. [PubMed: 7706029]
21. Grant MB, Khaw PT, Schultz GS, Adams JL, Shimizu RW. Effects of epidermal growth factor, fibroblast growth factor, and transforming growth factor-beta on corneal cell chemotaxis. Invest Ophthalmol Vis Sci 1992;33:3292–3301. [PubMed: 1428704]
22. Jester JV, Petroll WM, Cavanagh HD. Corneal stromal wound healing in refractive surgery: the role of myofibroblasts. Prog Retin Eye Res 1999;18:311–356. [PubMed: 10192516]
23. Huxlin KR, Yoon G, Nagy L, Porter J, Williams D. Monochromatic ocular wavefront aberrations in the awake-behaving cat. Vision Res 2004;44:2159–2169. [PubMed: 15183683]
24. Nagy LJ, MacRae S, Yoon G, et al. Photorefractive keratectomy in the cat eye: Biological and optical outcomes. J Cataract Refract Surg 2007;33:1051–1064. [PubMed: 17531702]
25. Bühren J, Yoon G, Kenner S, Macrae S, Huxlin K. The effect of optical zone decentration on lower- and higher-order aberrations after photorefractive keratectomy in a cat model. Invest Ophthalmol Vis Sci 2007;48:5806–5814. [PubMed: 18055835]
26. Jester JV, Huang J, Petroll WM, Cavanagh HD. TGFβ induced myofibroblast differentiation of rabbit keratocytes requires synergistic TGFβ, PDGF and Integrin signalling. Experimental Eye Research 2002;75:645–657. [PubMed: 12470966]
27. Jester JV, Barry-Lane PA, Cavanagh HD, Petroll WM. Induction of alpha-smooth muscle actin expression and myofibroblast transformation in cultured corneal keratocytes. Cornea 1996;15:505–516. [PubMed: 8862928]
28. Jester J, Barry P, Lind G, Petroll W, Garana R, HD C. Corneal keratocytes: in situ and in vitro organization of cytoskeletal contractile proteins. Invest Ophthalmol Vis Sci 1994;35:730–743. [PubMed: 8113024]
29. Radhakrishnan S, Rollins AM, Roth JE, et al. Real-time optical coherence tomography of the anterior segment at 1310 nm. Archives of Ophthalmology 2001;119:1179–1185. [PubMed: 11483086]
30. Wang J, Thomas J, Cox I, Rollins A. Noncontact measurements of central corneal epithelial and flap thickness after laser in situ keratomileusis. Investigative Ophthalmology and Visual Science 2004;45:1812–1816. [PubMed: 15161844]
31. Nagy LJ, MacRae S, Yoon G, Cox I, Huxlin KR. Photorefractive keratectomy in the cat eye: biological and optical outcomes. Journal of Cataract and Refractive Surgery 2007;33:1051–1064. [PubMed: 17531702]
32. Thibos LN, Applegate RA, Schwiegerling JT, Webb R. Standards for reporting the optical aberrations of eyes. J Refract Surg 2002;18:S652–660. [PubMed: 12361175]
33. Cheng X, Bradley A, Thibos LN. Predicting subjective judgment of best focus with objective image quality metrics. J Vis 2004;4:310–321. [PubMed: 15134478]
34. Jester JV, Barry-Lane PA, Cavanagh HD, Petroll WM. Induction of alpha-smooth muscle actin expression and myofibroblast transformation in cultured corneal keratocytes. Cornea 1996;15:505–516. [PubMed: 8862928]
35. Jester JV, Huang J, Barry-Lane PA, Kao WW, Petroll WM, Cavanaugh HD. TGFb-mediated myofibroblast differentation and a-smooth muscle actin expression in corneal fibroblasts requires actin re-organization and focal adhesion assembly. Investigative Ophthalmology and Vision Science 1999;40:1959–1967.
36. Beales MP, Funderburgh JL, Jester JV, Hassell JR. Proteoglycan synthesis by bovine keratocytes and corneal fibroblasts: maintenance of the keratocyte phenotype in culture. Investigative Ophthalmology and Vision Science 1999;40:1658–1663.
37. Jester JV, Huang J, Fisher S, et al. Myofibroblast differentiation of normal human keratocytes and hTERT, extended-life human corneal fibroblasts. Investigative Ophthalmology and Vision Science 2003;44:1850–1858.

38. Frank S, Madlener M, Werner S. Transforming growth factors beta1, beta2, and beta3 and their receptors are differentially regulated during normal and impaired wound healing. J Biol Chem 1996;271:10188–10193. [PubMed: 8626581]
39. Petroutsos G, Guimaraes R, Giraud JP, Pouliquen Y. Corticosteroids and corneal epithelial wound healing. Br J Ophthalmol 1982;66:705–708. [PubMed: 6896993]
40. Wilson SE, Mohan RR, Mohan RR, Ambrosio R, Hong JW, Lee JS. The corneal wound healing response: cytokine-mediated interaction of the epithelium, stroma and inflammatory cells. Progress in Retinal and Eye Research 2001;20:625–637. [PubMed: 11470453]
41. Nakamura K, Kurosaka D, Yoshino M, Oshima T, Kurosaka H. Injured corneal epithelial cells promote myodifferentiation of corneal fibroblasts. Investigative Ophthalmology and Vision Science 2002;43:2603–2608.
42. Nakamura K, Kurosaka D, Bissen-Miyajima H, Tsubota K. Intact corneal epithelium is essential for the prevention of stromal haze after laser in situ keratomileusis. British Journal of Ophthalmology 2001;85:209–213. [PubMed: 11159488]
43. Nakamura K. Interaction between injured corneal epithelial cells and stromal cells. Cornea 2003;22:S35–S47. [PubMed: 14703706]
44. Møller-Pedersen T. Keratocyte reflectivity and corneal haze. Exp Eye Res 2004;78:553–560. [PubMed: 15106935]
45. Møller-Pedersen T, Cavanagh HD, Petroll WM, Jester JV. Neutralizing antibody to TGFbeta modulates stromal fibrosis but not regression of photoablative effect following PRK. Current Eye Research 1998;17:736–747. [PubMed: 9678420]
46. Jester J, Barry-Lane P, Petroll W, Olsen D, HD C. Inhibition of corneal fibrosis by topical application of blocking antibodies to TGF beta in the rabbit. Cornea 1997;16:177–187. [PubMed: 9071531]
47. Seiler T, Kaemmerer M, Mierdel P, Krinke HE. Ocular optical aberrations after photorefractive keratectomy for myopia and myopic astigmatism. Arch Ophthalmol 2000;118:17–21. [PubMed: 10636408]
48. Jester J, Petroll W, Barry P, Cavanagh H. Temporal, 3-dimensional, cellular anatomy of corneal wound tissue. J Anat 1995;186:301–311. [PubMed: 7649828]
49. Yoon G, MacRae S, Williams DR, Cox IG. Causes of spherical aberration induced by laser refractive surgery. Journal of Cataract and Refractive Surgery 2005;31:127–135. [PubMed: 15721705]
50. Kersey JP, Broadway DC. Corticosteroid-induced glaucoma: a review of the literature. Eye 2006;20:407–416. [PubMed: 15877093]

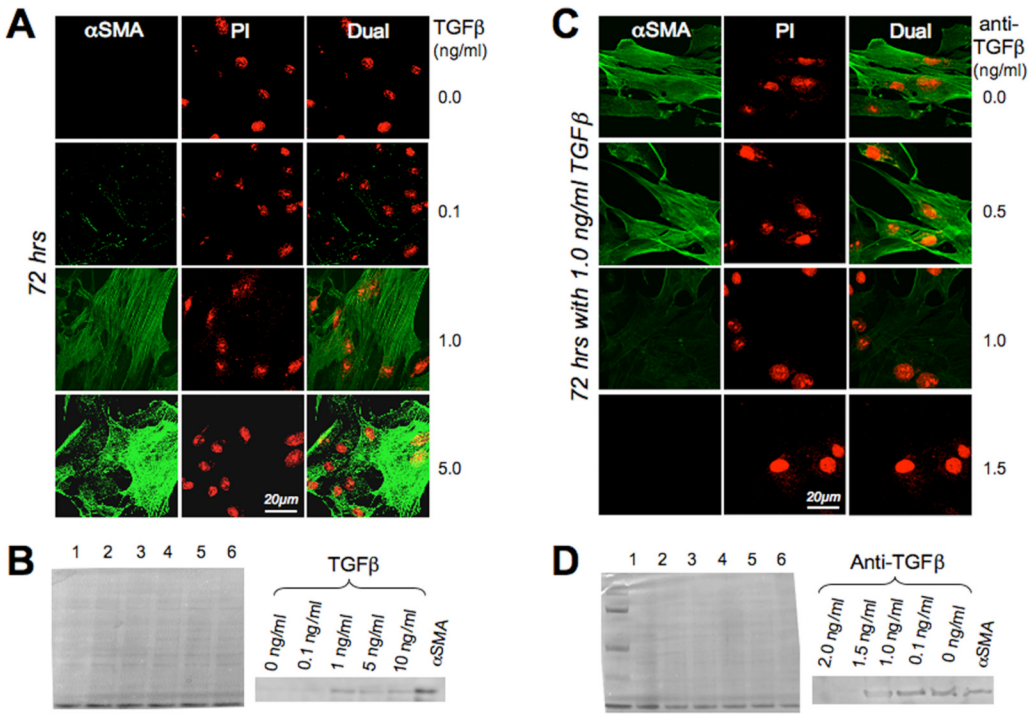

Figure 1. Cell culture results

A. Photomicrographs of feline corneal keratocytes cultured for 72 hrs in serum free defined medium supplemented with different concentrations of TGFβ. Cells are double-labeled with propidium Iodide (PI) and antibodies against αSMA (green). Note the strong αSMA immunoreactivity of cells exposed to 1 and 5 ng·mL^{-1} $_{TGF}$β. **B.** Western blots of feline corneal keratocytes cultured for 72 hrs in serum free defined medium supplemented with different concentrations of TGFβ. The left-most blot is a Coomassie stain demonstrating equal protein load in each lane. Lanes 1, 2, 3, 4 and 5 were loaded with keratocytes exposed to 0, 0.1, 1, 5 and 10 ng·mL^{-1} of TGFβ respectively. Lane 6 was loaded with pure αSMA protein as a control. The right blot shows anti-αSMA staining of the same blot, and demonstrates increasing amounts of αSMA protein in keratocytes cultured with increasing concentrations of TGFβ. **C.** Photomicrographs of feline corneal keratocytes cultured for 72 hrs in serum free defined medium containing 1 ng·mL^{-1} TGFβ and supplemented with different concentrations of anti-TGFβ antibodies. Staining was as in A. Note the strong αSMA immunoreactivity of cells cultured with 1 ng·mL^{-1} TGFβ and up to 0.5ng·mL^{-1} of anti-TGFβ. At anti-TGFβ concentrations of 1 or 1.5 ng·mL^{-1}, αSMA expression was strongly inhibited. **D.** Western blots of feline corneal keratocytes cultured for 72 hrs in serum free defined medium containing 1 ng·mL^{-1} TGFβ and different concentrations of anti-TGFβ antibodies. The left-most blot is a Coomassie stain demonstrating equal protein load in each lane, as well as a reference ladder (leftmost lane). Lanes 1, 2, 3, 4 and 5 were loaded with keratocytes cultured for 72 hrs in serum-free defined medium containing 1 ng·mL^{-1} TFGβ and 2.0, 1.5, 1, 0.1 or 0 ng·mL^{-1} of anti-TGFβ antibody respectively. Lane 6 was loaded with pure αSMA protein as a control. The right blot shows anti-αSMA staining of the same Western blot, and demonstrates decreasing amounts of αSMA protein in keratocytes cultured with increasing concentrations of anti-TGFβ antibody.

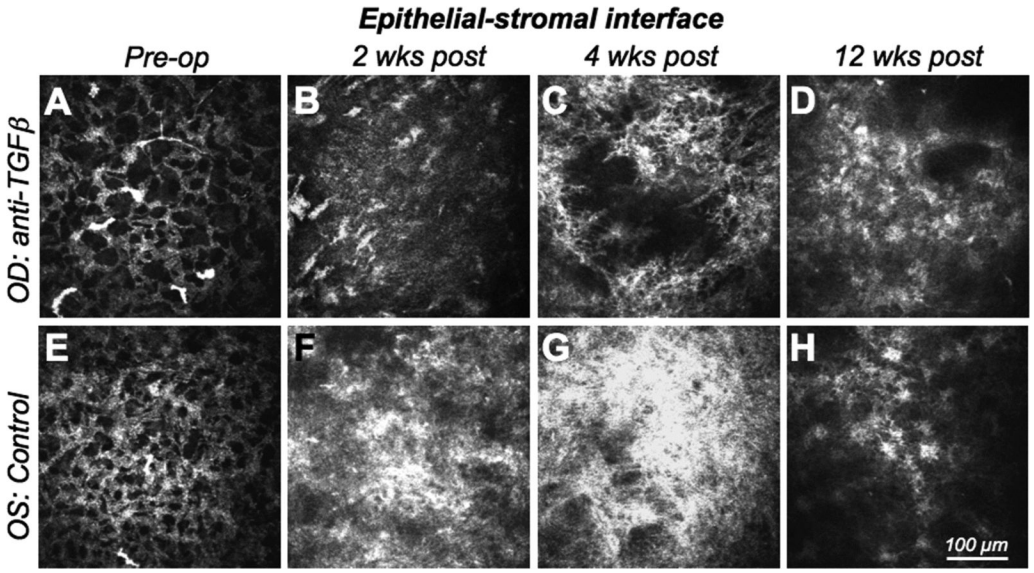

Figure 2. In vivo confocal imaging of the epithelial-stromal interface

A-D. Images of the right eye (OD) of one cat treated with anti-TGFβ/Dexamethasone after PRK. Images were collected pre-operatively, 2, 4 and 12 weeks post-operatively, and demonstrate the radical change in reflectivity in this corneal region over time. **E-F**. Images of the left eye (OS) of the same cat, which only received vehicle solution following −10D PRK. Images were also collected pre-operatively, and then at 2, 4 and 12 weeks following PRK. Note the well-organized, regular syncitium of quiescent keratocytes pre-operatively and the disrupted, reactive and strongly reflective activated keratocytes and myofibroblasts that replace it postoperatively. Note also that the control eye exhibits much stronger reflectivity and cellularity than the anti TGFβ-treated eye, especially at 2 and 4 weeks post PRK.

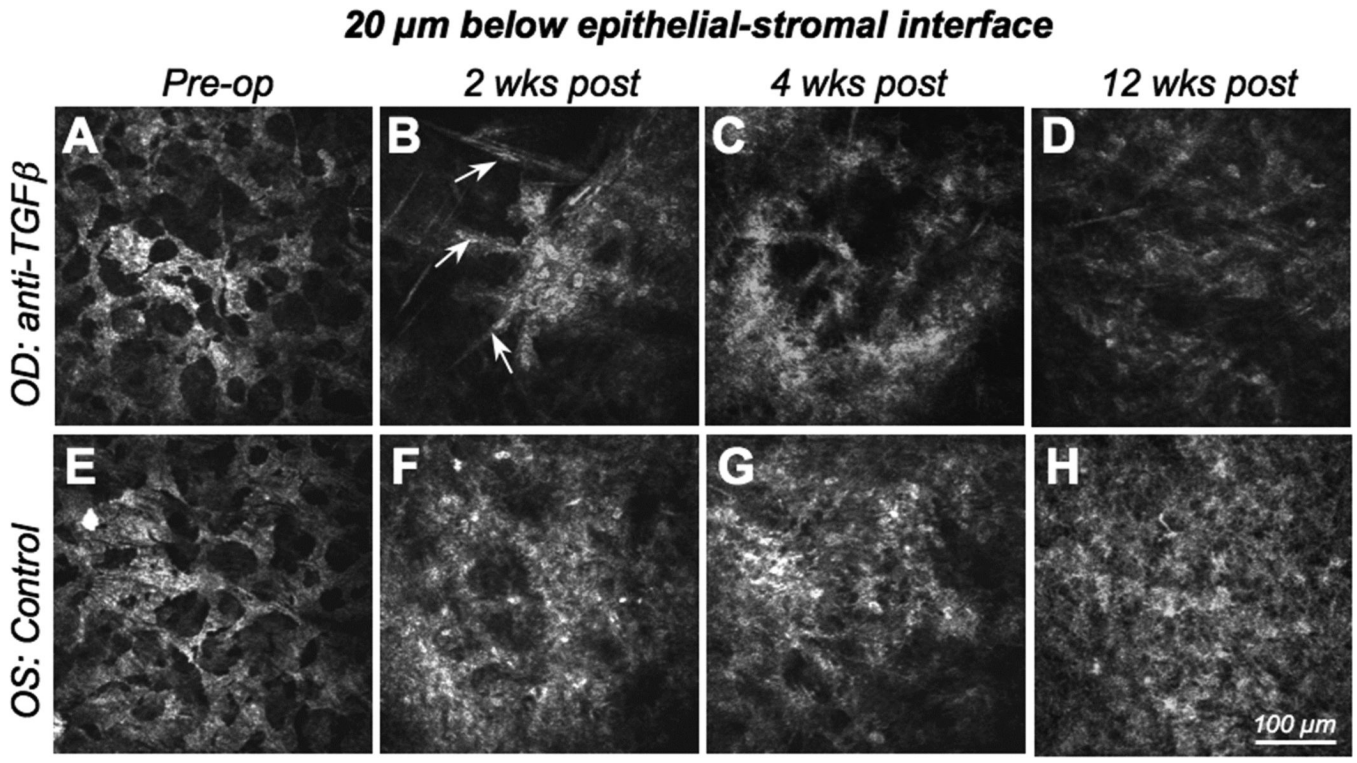

Figure 3. In vivo confocal imaging 20µm below the epithelial-stromal interface

A-D. Images of the right eye (OD) of the cat in Fig.2, which was treated with −10D PRK and anti-TGFβ/Dexamethasone post-operatively, and demonstrating the radical change in reflectivity in this corneal region over time. **E-F**. Images of the left eye (OS) of the same cat, which only received vehicle solution following the −10D PRK. Images were also collected preoperatively, and then at 2, 4 and 12 weeks following PRK. Note the well-organized, regular syncitium of quiescent keratocytes pre-operatively, which contrasts with the less regular, reactive and strongly reflective activated keratocytes and myofibroblasts that replace it postoperatively, particularly in the control (left) eye. Indeed, the control eye exhibits much stronger reflectivity and cellularity than the anti-TGFβ-treated eye, especially at 2 and 4 weeks post-PRK. Note the spindle-shaped migratory fibroblasts (arrowed) and the cluster of reflective activated keratocytes in the right eye at 2 weeks post-PRK. Clustering is still present in anti-TGFβ-treated eyes 4 weeks post-PRK and is not seen in control eyes. As is evident in this set of images, control eyes exhibited greater cell density and greater reflectivity at this corneal depth than eyes treated with anti-TGFβ/Dexamethasone, at all post-operative time points.

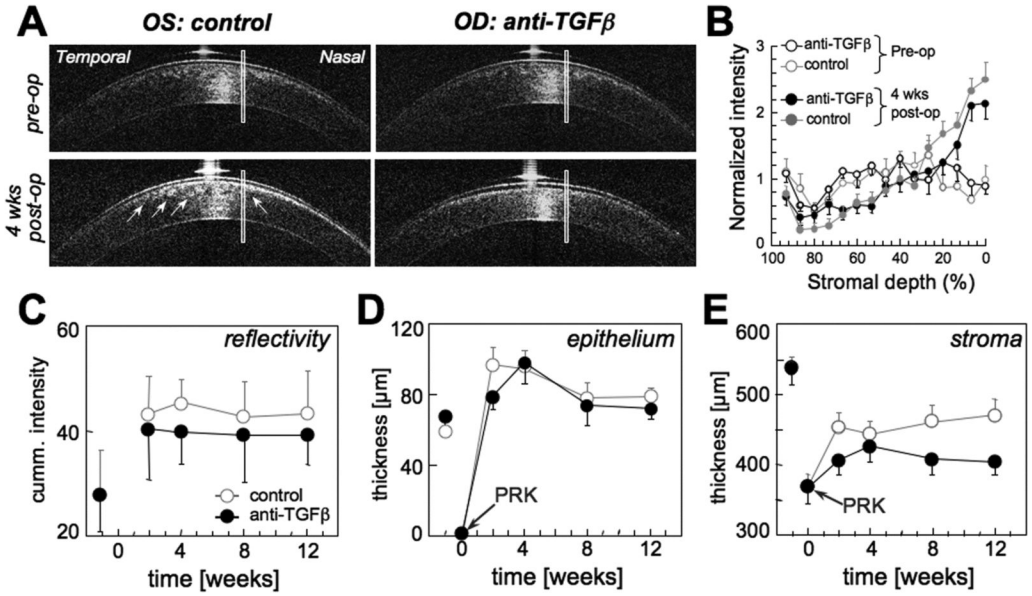

Figure 4. Effect of anti-TGFβ treatment on corneal reflectivity and thickness, as measured with optical coherence tomography(OCT)

A. OCT images of the left (OS) and right (OD) corneas of a cat before and 4 weeks after −10D PRK. Note the greater reflectivity in the sub-ablation stroma of the control eye (arrows) relative to the eye that received anti-TGFβ treatment post-PRK. The rectangles superposed over the corneal images indicate the location and approximate size of the areas analyzed for reflectivity and thickness. These analysis areas were located 1mm nasal to the center of each cornea and well outside the zone of the specular reflex. **B.** Plot of normalized backscattered light intensity obtained from the rectangular analysis areas in 25 OCT images of the left and right corneas of the cat shown in A versus central stromal depth, expressed as a percentage of the total stromal depth. 0% indicates the stromal/endothelial boundary, while 100% indicates the stromal/epithelial boundary. Reflectivity profiles are shown for both eyes of this cat pre-operatively and 4 weeks post-PRK. Note that the curves are relatively flat for both eyes pre-operatively, but that stromal reflectivity increases post-PRK. However, the eye that received anti-TGFβ treatments exhibits lower anterior stromal reflectivity than the control eye. **C.** Plot of the area under the reflectivity curve (see examples of these in B) for the anterior 20% of the corneal stroma as a function of time. Eyes that received anti-TGFβ treatment post-PRK exhibited lower mean reflectivity than control eyes at all post-operative time-points. **D.** Central epithelial thickness for control and anti-TGFβ eyes as a function of time. There was no significant difference between the two treatment groups. **E.** Central stromal thickness for control and anti-TGFβ eyes as a function of time, illustrating the consistently thinner stromas in anti-TGFβ treated eyes across post-PRK time-points. All graphs show means and standard errors of the mean.

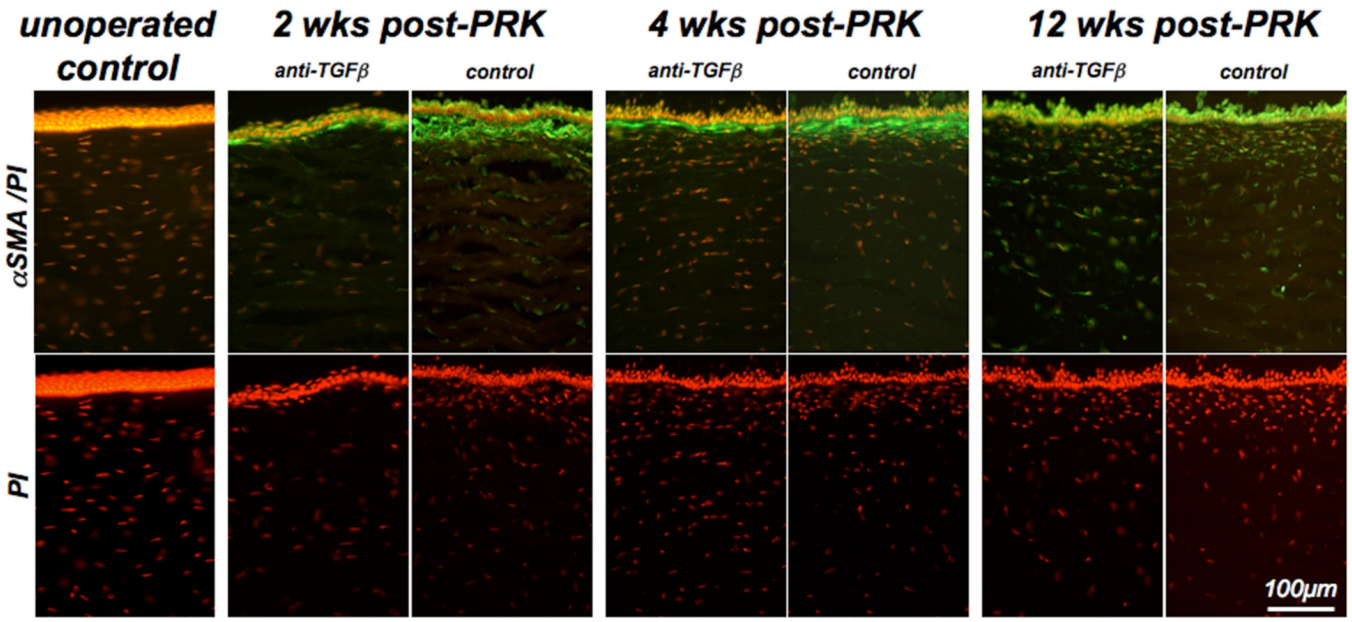

Figure 5. Effect of anti-TGFβ treatment on αSMA expression and stromal cell density

Photomicrographs of corneal sections from a normal, unoperated cat and pairs of cat eyes that underwent PRK and received either vehicle or anti-TGFβ treatment post-operatively. These cats were sacrificed at 2, 4 and 12 weeks post-PRK and sections of their corneas were double-labeled with antibodies against αSMA to label myofibroblasts and with propidium iodide (PI) to label cell nuclei. Note the absence of αSMA staining in the operated cat cornea, in contrast with the significant αSMA expression in the sub-ablation stroma of eyes that underwent PRK. The band of αSMA expression was significantly thicker and more continuous in control eyes than in contralateral eyes treated with anti-TGFβ. It was also most intense at 2 and 4 weeks post-PRK, becoming almost absent in the stroma by 12 weeks-post-PRK. PI staining also revealed an area of increased cellularity under the ablation zone in all post-operative eyes, although cell density appeared consistently higher in control eyes relative to eyes treated with anti-TGFβ.

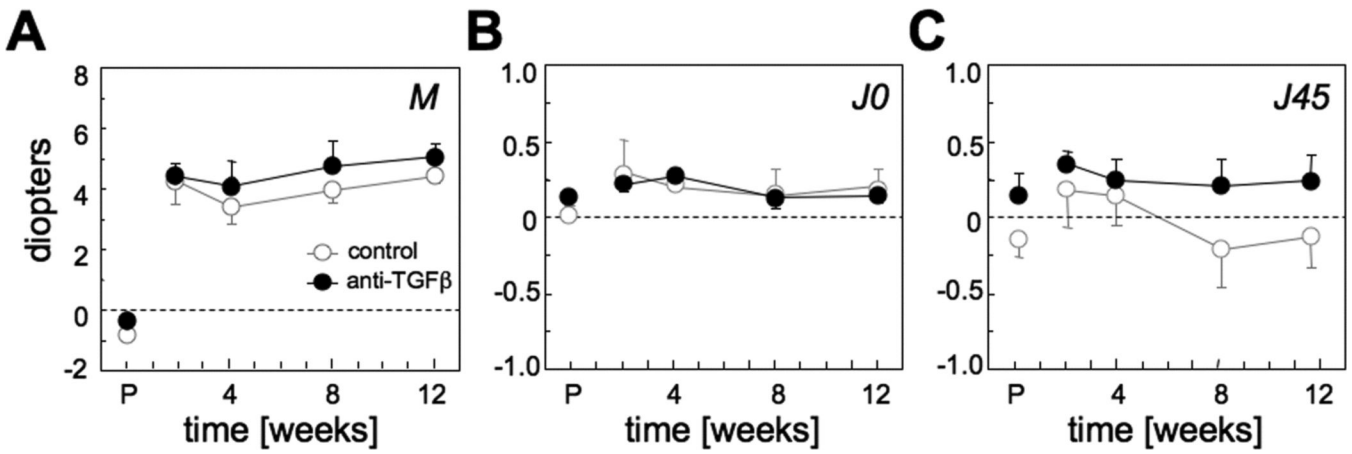

Figure 6. Effect of anti-TGFβ treatment on lower-order ocular aberrations

A. Spherical equivalent *M*. **B.** 0°/90° astigmatic component *J0*. **C.** 45°/135° astigmatic component *J45*. All graphs are plotting values expressed as dioptric power vectors *M*, *J0* and *J45* for a 6 mm pupil diameter as a function of post-operative time. All values are means and standard errors of the mean. On the horizontal axis, P=pre-operative time. Note that lack of significant effect of anti-TGFβ treatment on changes in lower order aberrations induced by PRK.

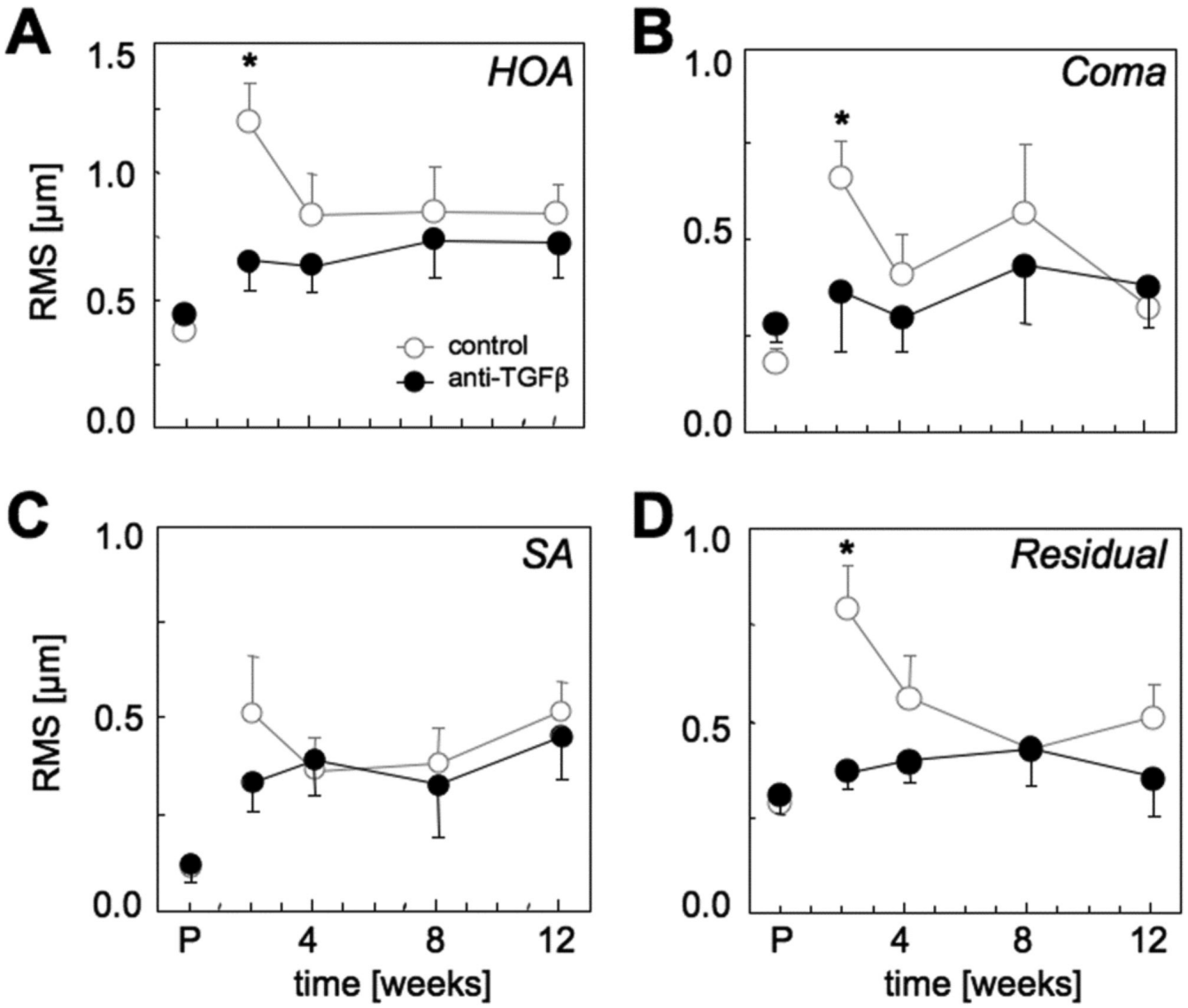

Figure 7. Effect of anti-TGFβ treatment on higher order ocular aberrations

A. Total higher order aberration (HOA) RMS. **B.** Coma RMS (RMS of all $C_n^{\pm 1}$). **C.** Spherical aberration (SA) RMS (RMS of all C_n^0). **D.** Residual HOA RMS (RMS of all $C_n^{\geq|\pm 2|}$). All graphs are plotting means ± standard errors of the mean as a function of post-operative time, with P=pre-operative time. * = significantly greater change from pre-op in controls than eyes that received anti-TGFβ treatment at that particular time-point ($P<0.05$). Note the peak in HOA, coma, spherical aberration and residual HOA exhibited by control eyes 2 weeks post-PRK. Except for spherical aberration RMS, anti-TGFβ treated eyes maintained pre-operative levels of higher order aberrations after PRK.

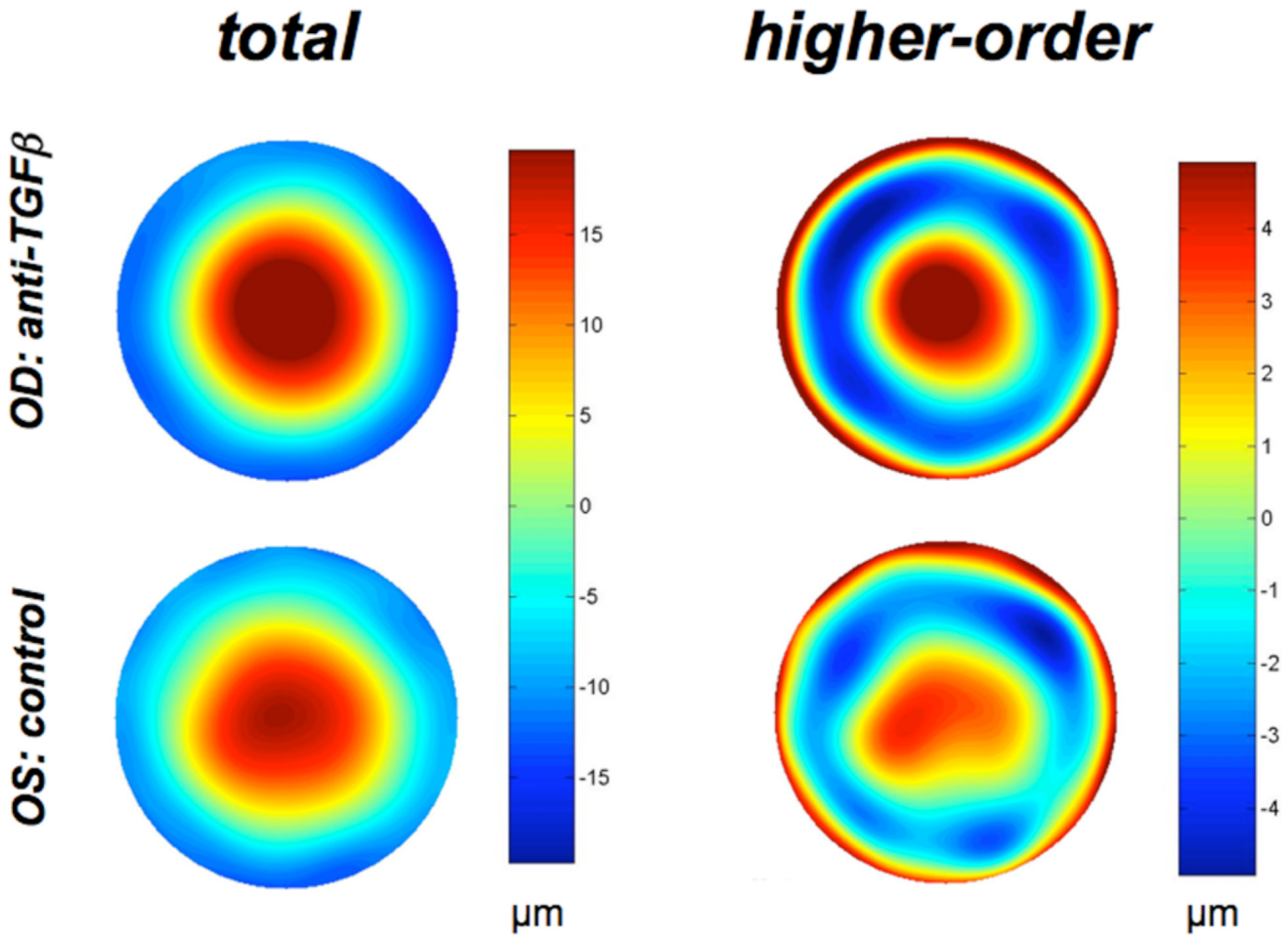

Figure 8. Anti-TGFβ treatment causes spatial smoothing of higher order optical aberrations post-PRK

Wavefront error maps (for a 9mm pupil diameter) in the right and left eye of the same cat at 8 weeks post-PRK, demonstrating the greater spatial irregularity of the wavefront in the control eye (bottom) compared to the eye treated with anti-TGFβ after PRK. While this effect was greatest at 2 weeks post-PRK, it was also maintained over the longer term.

Table 1

In vivo experiment
eyes, treatments and measures

	# PRK-treated eyes undergoing					
	Exclusion from study	***OCT***	***In vivo confocal***	***Histology***	***Wavefront sensing***	**Total**
Anti-TGFβ treatment	*3*	*10*	*2*	*8*	*4*	13
Control	*1*	*15*	*2*	*10*	*7*	16

Table 2

Treatment effects at 2 weeks post-PRK

shown as change of refraction, VSOTF and higher-order aberrations for a 6mm pupil diameter relative to baseline. All data are expressed as means and standard deviations (minima and maxima in parentheses). Data in bold exhibit statistically significant differences between control eyes and those that received anti-TGFβ treatment.

	anti-TGFβ (n=4)	**controls (n=7)**
M (spherical equivalent) [D]	4.79 ±0.86 (4.04 to 5.68)	5.04 ±2.11 (2.56 to 7.65)
J0 (0/90° astigmatism) [D]	0.09 ±0.09 (−0.03 to 0.20)	0.27 ±0.48 (−0.38 to 0.84)
J45 (45/135° astigmatism)[D]	0.20 ±0.13 (0.05 to 0.37)	0.30 ±0.52 (−0.20 to 1.14)
total HOA RMS [μm]	**0.20±0.18**† **(0.036 to 0.362)**	**0.82±0.32 (0.477 to 1.232)**
coma RMS [μm]	**0.08 ±0.28*** **(−0.13 to 0.46)**	**0.48 ±0.22 (0.17 to 0.71)**
spherical aberration RMS [μm]	0.21 ±0.07 (0.139 to 0.279)	0.41 ±0.40 (−0.136 to 1.001)
residual HOA RMS [μm]	**0.06 ±0.1**† **(−0.025 to 0.201)**	**0.49 ±0.27 (0.196 to 0.874)**
6^{th} to 10^{th} order RMS [μm]	0.01 ±0.01 (−0.022 to 0.297)	0.10 ±0.09 (0.014 to 0.235)
log BCVSOTF	−0.27 ±0.34 (−0.65 to 0.18)	−0.67 ±0.27 (−1.15 to −0.46)

BCVSOTF: visual Strehl ratio, based on the optical transfer function (simulation for best spectacle correction)

total RMS: RMS of 2^{nd} to 5^{th} order aberrations

HOA RMS: RMS of 3^{rd} to 5^{th} order aberrations

coma RMS: RMS of 3^{rd} and 5^{th} order coma terms

residual HOA RMS: RMS of all non-coma, non-spherical HOA

* P <0.05 (inter-group differences Student's t test)

† P <0.01 (inter-group differences Student's t test)